44. BASEMENT PALEOMAGNETISM OF HOLE 504B[1]

Toshio Furuta, Ocean Research Institute, University of Tokyo, Tokyo, Japan
and
Shaul Levi, School of Oceanography, Oregon State University, Corvallis, Oregon

ABSTRACT

Paleomagnetic and rock magnetic measurements of basalt specimens from DSDP Hole 504B, associated with the Costa Rica Rift, have a mean natural remanence intensity ($\overline{J}_n$) between 5 and 10×10^{-3} gauss, consistent with the presence of a magnetized layer that is 0.5 to 1 km thick, which produces the observed magnetic anomalies. A mean Koenigsberger ratio ($\overline{Q}_n$) greater than 10 indicates that the remanence dominates the magnetic signal of the drilled section. The susceptibility (χ) increases with depth, and the median demagnetizing field (MDF) decreases with increasing depth in Hole 504B, congruent with the downhole increase in the relative abundance of massive flow units. Hole 504B is composed of at least 12 units with distinct stable average inclinations ($\overline{I}_s$), which probably represent extrusion at times of different geomagnetic field directions and possibly also the effects of faulting. The thickness of basalt associated with these inclination units varies from less than 9 meters to possibly as much as 160 meters. Two relatively thick magnetic units (40 m and 45 m, separated by 100 m) have anomalously high $\overline{I}_s$ values of $-53°$ and $-63°$, in contrast with the near zero inclinations expected for the equatorial latitude of Site 504. For this reason and because the average inclination of all the magnetic units is skewed to a negative value, it might be that the entire section at Hole 504B was tilted by approximately 30°.

INTRODUCTION

Hole 504B was drilled at 1°13.63′N and 83°43.81′W, a position south of the Costa Rica Rift, in oceanic basement that was extruded about 5.9 m.y. ago at a time when the earth's magnetic field was reversely magnetized (see Site 504 chapter, this volume). Hole 504B was begun during Leg 69, when the basement's upper 214 meters were cored; during Leg 70, the site was reoccupied and an additional 347.5 meters of basalt were cored. The basement section consists of alternating pillow lavas and massive flows. This report presents the combined paleomagnetic results and some rock magnetic data for Hole 504B.

MEASUREMENT TECHNIQUES

Remanent magnetization was measured on a Digico spinner magnetometer; alternating field (AF) demagnetization was carried out on a Schonstedt Instrument Co. single-axis geophysical sample demagnetizer, and low-field susceptibility was measured with a Bison Instrument, Inc. susceptibility meter.

RESULTS AND DISCUSSION

Intensity of Natural Remanent Magnetization

J_n, the intensity of natural remanent magnetization (NRM), is highly scattered, ranging more than two orders of magnitude from less than 0.1 to nearly 30×10^{-3} gauss (Table 1). Such wide variation is not unusual in other DSDP-drilled basalts from normal ocean crust (Ade-Hall and Johnson, 1976; Hall and Ryall, 1977; Lowrie, 1977; Marshall, 1978; Day et al., 1979; Levi et al., 1980). There is no apparent depth dependence of J_n (Table 1, Table 2, and Fig. 1). Rather, the variation of J_n depends on whether the basement rock is fine or coarse grained, with the higher J_n values generally associated with the finer-grained igneous rocks, such as pillows and the chilled margins of massive flows. In Table 3 we compare the magnetic properties of the pillow lavas and massive flows. The pillows have $\overline{J}_n$ values twice those of the massive flows—10.2 versus 4.7×10^{-3} gauss, respectively. The single most representative average value for J_n of Hole 504B is between 5 and 10×10^{-3} gauss, depending on the method of averaging. This result is consistent with the calculations of Klitgord et al. (1975), who determined magnetization intensities for a 0.5-km source layer by inverting near-bottom magnetic profiles across reversal boundaries. For Costa Rica Rift basalts aged 4 to 5 m.y., they obtain a value for magnetization intensity of about 5×10^{-3} gauss. Because the recovery at Hole 504B was poor (average: 26%), the true $\overline{J}_n$ value is not known. It could be considerably higher or lower than shown by our measurements, depending on whether the unrecovered material is chiefly composed of pillow basalts (which have a comparatively high value of $\overline{J}_n$) or breccia and more altered material (which have a comparatively low value of $\overline{J}_n$).

Initial Susceptibility

The value of initial susceptibility, χ, is controlled primarily by the volume concentration of ferrimagnetic minerals and their grain size. Both higher concentrations of ferrimagnetic material and larger grain size cause χ to increase. In basalts from Hole 504B, χ varies from 0.3 to 6.1×10^{-3} gauss/Oe (Table 1). The effect of grain size on χ is shown in Table 3, where $\overline{\chi}$ is 1.4×10^{-3} gauss/Oe for the finer-grained pillow lavas and 2.4×10^{-3} gauss/Oe for the coarser massive flows. Similar distinctions between pillow lavas and massive flows occur in submarine basalts in the Atlantic Ocean, particu-

[1] Cann, J. R., Langseth, M. G., Honnorez, J., Von Herzen, R. P., White, S. M., et al., *Init. Repts. DSDP*, 69: Washington (U.S. Govt. Printing Office).

Table 1. Paleomagnetic properties of specimens from Hole 504B.

Magnetic Unit	Sample (interval in cm)	Sub-bottom Depth (m)	J_n (10^{-3} gauss)	I_s (°)	χ (10^{-3} gauss/Oe)	Q_n	MDF (Oe)
1a	504B-3-1, 87-89	278.9	4.2	−11	1.8	8	120
	3-1, 108-110	279.1	7.1	3	1.5	14	110
1b	4-1, 108-110	281.1	9.5	−18	0.6	47	260
	4-2, 101-103	282.5	21.1	−17	0.8	77	240
	4-3, 122-124	284.2	15.1	−15	0.6	76	400
	4-4, 41-43	284.9	7.4	−3	1.2	17	210
	4-5, 124-126	287.2	10.7	−16	1.0	32	230
	5-1, 57-59	290.1	12.8	−9	1.0	38	170
	5-2, 41-43	291.4	17.6	−15	0.8	66	180
	6-1, 55-57	299.1	9.2	−12	0.4	66	430
	6-2, 36-38	300.3	5.0	−12	1.5	10	145
1c	7-1, 33-35	307.8	11.7	−6	0.3	108	550
	7-2, 98-100	310.0	14.7	(−9)	0.6	70	—
	7-3, 127-129	311.8	12.0	−5	1.1	30	120
	7-4, 35-37	312.3	8.9	−5	1.3	19	130
	7-5, 3-5	313.5	8.6	−6	1.6	16	100
	8-1, 59-61	317.1	1.6	−12	1.5	3.2	75
	8-2, 86-88	318.9	6.2	−6	1.6	11	110
	8-3, 73-75	321.7	4.2	−7	1.6	8	115
	8-4, 58-60	322.6	5.4	0.4	1.4	11	110
1d	9-1, 51-53	327.1	28.8	−14	0.8	100	200
	9-2, 73-75	332.2	3.1	−15	1.5	6	130
2a	10-2, 11-13	337.7	3.0	−41	1.5	6	140
	11-1, 19-21	343.7	0.5	−30	1.0	1.3	180
	11-2, 76-78	345.7	0.8	−32	1.1	2.1	160
	11-3, 27-29	346.8	0.8	32?	1.0	2.4	170
	12-1, 50-52	353.0	2.1	−31	1.3	4.7	160
	12-2, 107-109	355.1	1.0	−29	1.4	2.1	170
	13-1, 140-142	362.9	0.8	−19	1.2	2	180
	13-2, 100-102	364.0	2.0	(−21)	1.4	4	—
	13-3, 71-73	365.2	4.5	−31	1.8	7	140
	13-4, 15-17	366.1	4.1	−30	1.6	8	80
	14-1, 39-41	370.9	7.0	−29	1.5	13	160
	15-2, 26-28	376.8	1.2	−32	1.3	2.8	160
	15-3, 138-140	379.4	1.7	−24	1.7	2.8	150
	15-4, 129-131	380.8	5.7	−31	1.3	12	180
	15-5, 52-54	381.5	2.6	−23	1.7	4.6	125
	16-1, 20-22	384.2	2.2	−24	1.6	4	130
	16-2, 6-8	385.6	0.8	−30	1.6	1.5	180
	16-3, 66-68	387.7	0.2	−34	2.0	0.6	240
	16-3, 134-136	388.3	6.5	−40	1.4	13	150
	16-4, 105-107	389.6	7.0	(−27)	0.9	21	—
2b	17-1, 96-98	394.0	4.7	−12	1.5	9	160
	17-2, 104-106	395.5	6.5	17?	1.4	13	145
	18-1, 71-73	398.7	13.8	−23	1.4	28	110
	19-1, 101-103	404.0	7.0	−25	0.6	33	210
	19-2, 86-88	405.4	2.8	−10	1.6	5	125
2c	20-1, 109-111	413.1	2.5	−31	1.5	4.5	105
	21-1, 137-139	422.4	2.1	−34	1.7	3.4	145
	21-2, 57-59	423.1	10.8	(−28)	1.3	24	—
	21-3, 123-125	425.2	3.5	−29	1.7	6	90
	21-4, 136-138	426.8	3.7	−26	1.7	6	170
	22-1, 62-64	430.6	4.3	−27	0.7	18	370
	23-1, 88-90	439.9	4.9	−40	1.6	8	160
	24-1, 100-102	449.0	6.5	−29	1.1	16	170
	24-2, 62-64	450.1	6.3	−36	0.9	20	180
	24-3, 76-78	451.8	5.8	−29	1.3	13	180
	25-2, 83-85	459.4	0.7	−25	2.4	0.9	110
2d	27-1, 109-111	467.1	0.9	−7	2.4	1.1	85
	27-2, 106-108	468.6	4.5	−16	1.0	14	200
	28-1, 95-97	476.0	3.3	−10	2.3	4.3	60
2e	28-3, 56-58	478.6	4.4	−46	1.7	8	160
	28-4, 123-125	480.7	0.4	−43	2.7	0.4	200
	29-1, 4-6	484.0	6.2	−20	1.3	14	140
	32-1, 24-26	507.8	2.9	−46	1.4	6	165
	32-1, 49-51	508.0	5.1	−45	3.2	5	88
	32-1, 96-98	508.5	6.4	−35	3.3	6	86
	32-2, 19-21	509.2	8.4	−14	2.4	10	141
	32-2, 55-57	509.6	8.6	−29	2.5	11	140
3	33-1, 73-75	517.2	14.2	4	2.2	19	89
	33-2, 126-128	519.3	18.2	15	2.2	26	111
	34-2, 118-120	528.2	14.7	7	1.5	29	152
4	35-1, 44-46	535.0	5.5	−31	1.4	12	90
	35-1, 109-112	535.6	3.5	−36	0.3	34	374
	35-1, 116-118	535.7	5.1	−27	1.1	14	178
	35-2, 42-44	536.4	2.8	−28	1.4	6	95
	35-2, 53-56	536.5	4.4	−36?	1.1	13	110
	36-1, 78-80	544.3	1.8	−30	2.6	2.1	54
	36-2, 68-70	545.7	0.8	−26	2.4	1.0	99
	36-3, 101-103	547.5	2.7	−26	2.5	3.3	60
	37-1, 115-117	553.7	9.7	−31	2.0	14	101
	37-3, 51-54	556.0	3.0	−12	2.7	3.4	90

Table 1. (Continued).

Magnetic Unit	Sample (interval in cm)	Sub-bottom Depth (m)	J_n (10^{-3} gauss)	I_s (°)	χ (10^{-3} gauss/Oe)	Q_n	MDF (Oe)
5	504B-38-1, 84–86	562.3	10.4	6	—	—	128
	38-2, 110–113	564.1	8.9	10	—	—	92
	38-2, 129–131	564.3	11.0	15	2.9	11	94
	39-1, 48–50	571.0	7.6	−11?	2.1	11	89
	39-1, 104–107	571.6	2.5	7	3.4	2	66
	39-2, 118–120	573.2	4.0	6?	2.1	6	85
	39-2, 135–138	573.4	3.6	6	1.9	6	88
	40-1, 124–126	580.8	1.8	5	2.3	2.4	39
	40-3, 56–58	583.1	4.1	5	1.9	6	209
	41-1, 118–120	585.2	3.7	3	2.0	6	139
	41-3, 3–5	587.0	4.2	7	2.0	6	92
	41-3, 112–114	588.1	3.3	6	2.4	4.3	84
6	42-1, 97–99	594.0	3.1	−65	4.0	2.4	110
	42-2, 48–51	595.0	2.9	−62	3.2	2.8	129
	43-1, 66–69	602.7	0.1	−51	2.7	0.1	137
	43-2, 14–17	603.7	0.9	−79	2.8	1.0	89
	44-1, 22–25	611.2	7.6	−44	2.3	10	98
	44-2, 88–91	613.4	10.5	−49	2.3	14	88
	45-1, 118–121	621.2	2.2	−28	4.0	1.7	82
	46-1, 80–85	629.8	12.2	−47	2.2	17	105
7	47-2, 20–23	639.7	7.6	1	3.4	7	68
	47-2, 39–42	642.9	3.3	9	3.1	3.2	52
	48-1, 46–49	647.5	9.4	2	3.3	9	84
	48-2, 75–78	649.3	12.5	−2	2.9	13	88
8a	48-3, 82–85	650.8	6.6	−26	2.9	7	92
	49-1, 141–143	657.4	13.5	−34	2.0	20	133
	49-2, 18–20	657.7	6.4	−15	1.3	15	148
	49-3, 2–5	659.0	9.3	−31	3.0	9	102
8b	50-1, 28–30	665.3	27.7	−15	2.3	37	145
	51-1, 69–72	670.2	2.6	−17	2.5	3.1	109
	52-2, 128–131	681.3	2.7	−11	2.8	2.9	77
	52-4, 93–96	683.9	3.4	−8	2.5	4.1	75
8c	54-1, 64–66	692.6	4.7	−36	3.4	1.4	90
	55-2, 24–26	698.2	0.5	−34	4.1	0.4	79
	56-2, 66–68	707.7	3.4	−31	3.4	3.1	94
	57-1, 38–41	714.9	4.1	−19	4.1	3.0	76
	57-3, 108–111	718.6	1.1	−20	3.4	0.3	68
9	58-1, 30–32	723.8	1.9	8	3.5	2	147
	58-1, 88–90	724.4	3.2	11	3.2	3	80
	58-2, 20–23	725.2	1.3	7?	2.9	1.3	65
	58-2, 68–71	725.7	0.8	11?	3.6	0.7	56
	58-2, 80–83	725.8	0.5	13?	3.4	0.4	61
	58-3, 90–93	727.4	1.6	9?	3.2	1.5	69
10	60-1, 48–50	742.0	1.7	−21	3.1	1.7	114
	60-2, 41–44	743.4	13.8	−20	2.2	19	88
11	61-1, 89–92	751.4	19.9	−72	1.5	41	217
	61-3, 2–5	753.5	14.3	−27	1.9	23	182
	62-1, 124–127	756.3	25.0	−62	1.6	65	275
	62-2, 3–6	756.5	16.1	−82	3.1	16	130
	63-2, 89–92	766.4	7.0	−63	3.4	6	105
	63-4, 46–49	769.0	7.0	−69	4.6	4.6	65
	64.2, 129–132	775.8	8.5	−58	4.6	6	41
	65-1, 15–18	782.2	5.6	−67	3.3	5	77
12	66-2, 21–24	792.7	10.9	−37	3.9	8	82
	66-2, 58–61	793.1	1.7	−37	5.8	0.9	84
	69-1, 72–75	818.7	3.8	−32	6.1	1.9	61
	70-1, 95–98	828.0	1.6	−26	2.4	1.5	100
	70-1, 137–140	828.4	0.9	−35	3.9	0.7	101
	70-2, 9–12	828.6	1.6	−34	3.6	1.3	148

Note: Magnetic units were defined by the stable inclination. Inclinations in parentheses denote NRM values; question marks indicate doubtful sample orientation or somewhat questionable stable inclinations.

larly at DSDP Hole 417D (Levi, 1980). There is a definite increase in χ with increasing depth in Hole 504B (Fig. 1). This increase is probably related to the higher fraction of massive flow units deeper in the hole.

Koenigsberger Ratio

Koenigsberger ratio, Q_n, is the ratio of remanence to induced magnetization ($Q_n \equiv J_n/\chi h$, where h is the intensity of the ambient field). Only rarely is Q_n less than unity (Table 1), so the magnetic signal associated with Hole 504B is definitely dominated by the remanence (Table 2). As expected, Q_n values are generally positively correlated with J_n (Fig. 1). However, because of the progressive increase in χ with depth, the downhole profile of Q_n becomes more modulated and less similar to the J_n profile with increasing depth. Table 3 exhibits the very large difference between $\overline{Q}_n$ for the pillow basalts and the massive flow units; $\overline{Q}_n$ is 28 for the former and 7 for the latter. This difference is related to the fact that for a given volume of magnetic minerals, the specific intensity usually decreases and the susceptibility increases with increasing particle size. At Hole 504B this correlation is further enhanced by the superimposition of secondary remanence components, predominantly viscous

Table 2. Average magnetic properties of the magnetic units of Hole 504B.

Magnetic Unit	Core	Unit Thickness (m)	Number of Samples	J_n (10^{-3} gauss)	χ (10^{-3} gauss/Oe)	Q_n	MDF (Oe)	I_s (°)
1a	3	2	2	5.6 ± 2.1[a]	1.7 ± 0.2	11 ± 3	115 ± 7	−5 ± 7[b]
1b	4–6	27.5	9	12.0 ± 5.1	0.9 ± 0.3	48 ± 25	252 ± 100	−13 ± 5
1c	7–9	18	9	8.1 ± 4.2	1.2 ± 0.5	31 ± 35	164 ± 157	−6 ± 6
1d	9	9	2	16.0 ± 18.2	1.2 ± 0.5	53 ± 66	165 ± 50	−14 ± 0.2
2a	10–16	58.5	20	2.7 ± 2.3	1.4 ± 0.3	6 ± 5	159 ± 32	−30 ± 11
2b	17–19	19	5	7.0 ± 4.2	1.3 ± 0.4	18 ± 12	150 ± 39	−17 ± 7
2c	20–25	51	11	4.6 ± 2.7	1.4 ± 0.5	11 ± 8	168 ± 78	−30 ± 10
2d	27–28	12	3	2.9 ± 1.8	1.9 ± 0.8	7 ± 8	115 ± 75	−11 ± 5
2e	28–32	20	8	5.3 ± 2.8	2.3 ± 0.8	8 ± 4	140 ± 38	−35 ± 11
3	33–34	18	3	15.7 ± 2.2	2.0 ± 0.4	25 ± 5	117 ± 32	9 ± 6
4	35–37	27	10	3.9 ± 2.5	1.8 ± 0.8	10 ± 10	125 ± 94	−27 ± 7
5	38–41	29	12	5.4 ± 3.2	2.3 ± 0.5	6 ± 3	100 ± 43	5 ± 10
6	42–46	45	8	4.9 ± 4.6	2.9 ± 0.7	6 ± 7	105 ± 20	−53 ± 15
7	47–48	15	4	8.2 ± 3.8	3.2 ± 0.2	8 ± 4	73 ± 16	2 ± 5
8a	48–49	12	4	9.0 ± 3.3	2.3 ± 0.8	13 ± 6	119 ± 26	−30 ± 4
8b	50–52	22	4	9.1 ± 12.4	2.5 ± 0.2	12 ± 17	102 ± 33	−13 ± 4
8c	54–57	31	5	2.8 ± 1.8	3.7 ± 0.4	2 ± 1	81 ± 11	−28 ± 8
9	58	9	6	1.6 ± 1.0	3.3 ± 0.2	1.5 ± 0	80 ± 34	9 ± 2
10	60	9	2	7.8 ± 8.6	2.6 ± 0.6	10 ± 12	101 ± 18	−20 ± 1
11	61–65	40	8	12.9 ± 7.1	3.0 ± 1.3	21 ± 22	136 ± 82	−63 ± 16
12	66–70	45	6	3.3 ± 3.8	4.3 ± 1.4	2 ± 3	96 ± 29	−34 ± 4

[a] Uncertainties represent one standard deviation.
[b] Vector-mean inclination; the uncertainties represent one standard deviation of the arithmetic mean.

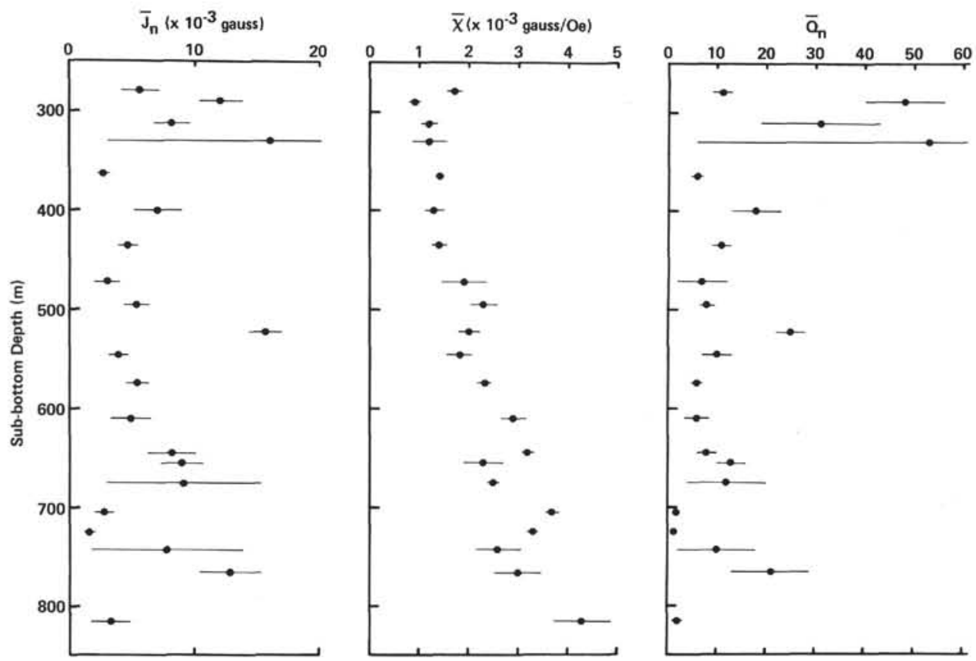

Figure 1. Downhole plots of $\overline{J}_n$, χ, $\overline{Q}_n$ for the inclination-defined magnetic units. Bars represent standard error, $\pm s/\sqrt{N}$).

Table 3. Average magnetic properties of pillow and massive flow basalts, Hole 504B.

	$\overline{J}_n$ (10^{-3} gauss)	$\overline{\chi}$ (10^{-3} gauss/Oe)	$\overline{Q}_n$	Number of Samples
Pillows	10.2 ± 6.9	1.45 ± 0.65	28.1 ± 27.4	40
Massive flows	4.7 ± 3.9	2.41 ± 1.08	7.4 ± 9.0	90

Note: Uncertainties represent one standard deviation.

remanence (VRM) during times of normal polarity fields, on a presumably reversed primary remanence. Such secondary remanences are relatively more significant for the coarser and magnetically less stable specimens, for which the value of J_n is preferentially reduced.

Median Demagnetizing Field

Median demagnetizing field, MDF, is the peak alternating field required to reduce the sample magnetization to half its initial value. MDF values were calculated from the AF demagnetization curves and are listed in Tables 1 and 2. In Figure 2, the $\overline{\text{MDF}}$ values decrease with increasing depth in Hole 504B, consistent with the increasing downhole fraction of massive flow units, which have larger grain size and less stable remanence than the finer-grained pillow lavas.

Stable Inclinations

Most of the specimens at Hole 504B were progressively demagnetized in alternating fields in increments

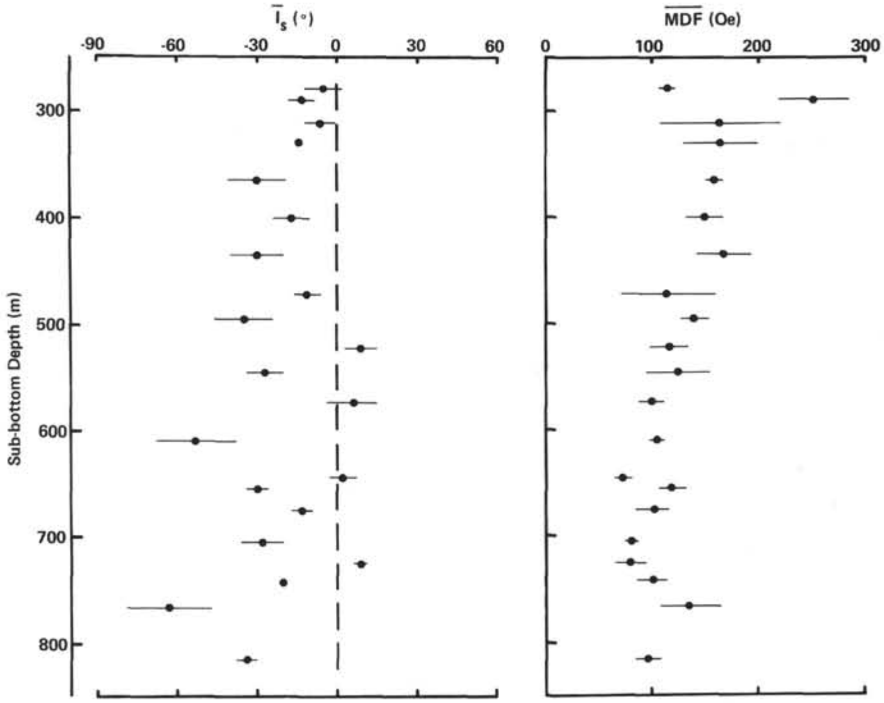

Figure 2. Downhole plots of $\overline{I}_s$ and $\overline{MDF}$ for the inclination-defined magnetic units. Uncertainties associated with $\overline{I}_s$ represent one standard deviation of arithmetic mean; uncertainties associated with $\overline{MDF}$ represent $\pm s/\sqrt{N}$).

no greater than 50 Oe until at least half the remanence was removed. Demagnetization usually proceeded until less than 10% of the remanence remained. Frequently, after the first demagnetization step at 25 Oe, there was an increase in the remanence intensity, and the stable inclinations were often more negative than the NRM values. Both these observations are consistent with the superposition of viscous remanence in a normal field (as in, for example, the present Brunhes Epoch) on reversed primary remanence. For most specimens the stable directions were well constrained. They were determined from the stable end points or clusters on the stereographic projection or from the plateaus of plots of inclination and declination versus peak AF values. Whenever possible, the stable directions were determined in the region comprising more than 10% of J_n. However, the demagnetization behavior of some specimens indicated the presence of secondary components to higher AF levels and to less than 10% of J_n. For a few specimens the effects of secondary remanence were never entirely removed, and in such cases the choice of stable directions was sometimes biased in favor of the more negative inclinations. Values of the stable inclinations (I_s) for individual specimens are listed in Table 1.

The stable inclinations are plotted versus depth in Figure 3. They were used to define the coherent magnetic units that appear there and in Tables 1 and 2. The units are entirely defined by I_s values, and they signify either hiatuses in volcanism of sufficient duration for the geomagnetic field to be represented by different inclinations or fault-block rotations. There are at least 12 distinct units in the cored column of Hole 504B. Units with the same Arabic numerals represent intervals that are defined by differences in stable inclination that are too slight for us to be certain that a separate unit should be defined. The thickness of the magnetic units varies from a single core (less than 9 m) to 7 cores (approximately 60 m). If Units 2a to 2e are combined, Unit 2 has a combined thickness of about 160 meters. Boundary zones between the magnetic units invariably also include lithologic boundaries, zones of brecciation, intervals of broken rocks, cooling margins, or transitions between zones of drastically different types of alteration. Comparison with glass composition data (Natland et al., this volume) indicates that the bases of Magnetic Units 2c, 3, 7, and 11 correspond to boundaries between basalts of different composition (separate eruptive units). The same is probably true of the bases of Magnetic Units 1a, 2b, 2e, 8a, 8b, and 8c as well, although glass data are sparse or lacking near these boundaries. However, the bases of Magnetic Units 1b, 1c, 1d, 2d, 4, 5, 6, and 9 are not associated with boundaries in glass composition, and Magnetic Unit 2a overlaps two glass types. The thickest chemically uniform glass unit is about 110 meters thick, and it is spread over four magnetic units.

Figures 2 and 3 show that the I_s values are skewed to negative inclination. Although the time-averaged inclination at Hole 504B is expected to be very near zero, it is in practice not possible to assess whether sufficient time is represented in the cored section to average out the full spectrum of geomagnetic secular variation. Thus, small deviations from the time-averaged field direction are most readily explained by the argument that the cored section does not represent the complete geomagnetic spectrum. If Magnetic Units 6 and 11 are excluded, the remaining magnetic units have an average inclination

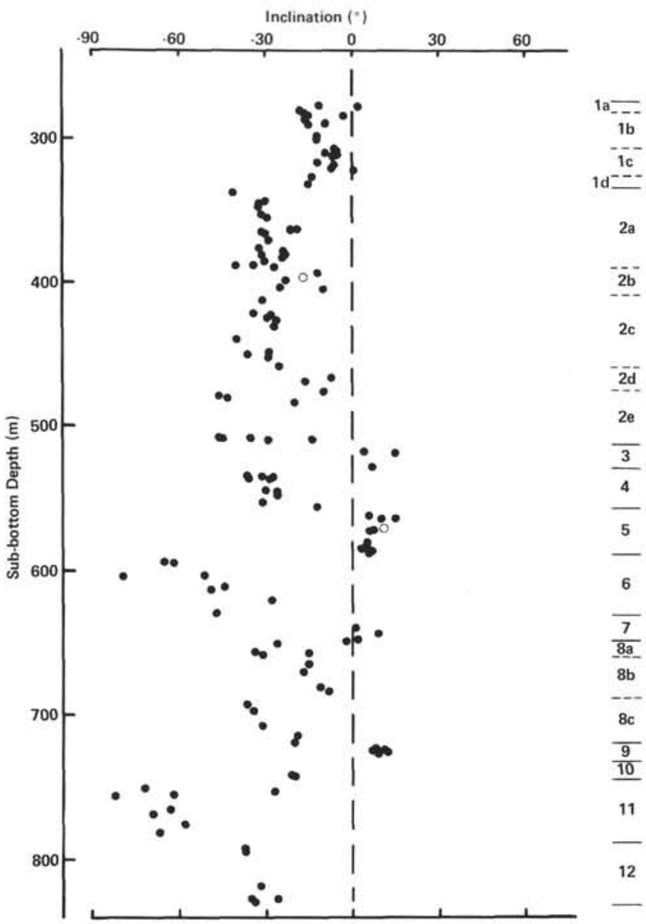

Figure 3. Downhole plot of stable inclinations for Hole 504B specimens. Open circles represent specimens thought to have been misoriented. Column on right shows the inclination-defined extrusive units. The present geomagnetic inclination at Hole 504B is 18.1°.

within 35° of the horizontal. Such inclinations might be caused by normal geomagnetic secular variations (SV). Units 6 and 11, however, have $\bar{I}_s$ values of $-53°$ and $-63°$, respectively, which exceed the fluctuations expected from normal SV. Furthermore, Units 6 and 11 both span approximately 45 meters (five cores), and they are separated by about 100 meters.

There are three possible explanations for the anomalous inclinations, but none is wholly satisfactory. First, the anomalous inclinations might be the result of anomalous geomagnetic excursions. However, two such excursions would be necessary to explain the inclinations of the two units, and both excursions would have had to be such as to produce steep negative inclinations. Second, the anomalous stable inclinations might represent a stable secondary remanence that may have accompanied the chemical alteration of rock units. However, Units 6 and 11 do not seem to exhibit a greater degree of alteration than the other units at Hole 504B. In addition, although low-temperature oxidation is known to reduce magnetization intensity drastically, there is no evidence that chemical change produces remanence oblique to the magnetic field that prevails during the time of chemical change. Third, tectonic rotation of about 30° about a west-trending horizontal axis might explain the anomalously steep inclinations. Since Hole 504B is on reversely magnetized crust, the rotation would have to be toward the ridge axis. Several small blocks could have rotated, but in that case the sense of rotation would have to be the same in both units (assuming that both units were formed while the field was reversely magnetized). A single rotation of the entire 550-meter crustal block by approximately 30° about a west-trending horizontal axis is an attractive explanation, because it would eliminate the anomalous inclinations and improve the symmetry of the section with respect to the expected 0° inclination. However, no near-surface crustal rotations of the order of 20 to 30° have been suggested by detailed geophysical surveys of the nearby Galapagos Spreading Center (Klitgord and Mudie, 1974), although no similar survey has been conducted north of Site 504, at the Costa Rica Rift. Of course, any combination of the above processes might have caused the anomalous inclinations.

SUMMARY

Paleomagnetic and rock magnetic studies of basalt specimens from DSDP Hole 504B, associated with the Costa Rica Rift, are summarized below.

1) The mean natural remanence intensity, $\bar{J}_n$, is between 5 and 10×10^{-3} gauss, consistent with the presence of a relatively uncomplicated magnetized layer 0.5 to 1 km thick which gives rise to the observed magnetic anomalies.

2) The mean Koenigsberger ratio, $\bar{Q}_n$, is greater than 10, indicating that the remanence dominates the magnetic signal of the drilled section.

3) The susceptibility, χ, increases with depth, and the median demagnetizing field, MDF, decreases with increasing depth in Hole 504B, consistent with the downhole increase in the relative abundance of massive flow units.

4) Hole 504B is represented by at least 12 units of distinct stable inclinations, I_s, which probably represent extrusion at times of different geomagnetic field directions and also possibly the effects of faulting. The thickness of basalt associated with these magnetic units of relatively uniform inclination varies from less than 9 meters to possibly as much as 160 meters.

5) Two relatively thick magnetic units (40 m and 45 m and separated by 100 m) have anomalously high I_s values of $-53°$ and $-63°$, in contrast with the near zero inclinations expected for the equatorial latitude of Site 504. For this reason and because the average inclination of all the magnetic units is skewed to a negative value, it might be that the entire section at Hole 504B was tilted by approximately 30°.

ACKNOWLEDGMENTS

This chapter was reviewed by H. P. Johnson, R. Karlin, J. H. Natland, and M. B. Steiner. This research was supported in part by the National Science Foundation Division of Ocean Science (OCE 79 19230).

REFERENCES

Ade-Hall, J. M., and Johnson, H. P., 1976. Paleomagnetism of basalts, Leg 34. *In* Yeats, R. S., Hart, S. R., et al., *Init. Repts. DSDP*, 34: Washington (U.S. Govt. Printing Office), 513-532.

Day, R., Halgedahl, S., Steiner, M., Kobayashi, K., Furuta, T., Ishii, T., and Faller, A., 1979. Magnetic properties of basalts from DSDP Leg 49. *In* Luyendyk, B. P., Cann, J. R., et al., *Init. Repts. DSDP*, 49: Washington (U.S. Govt. Printing Office), 781-791.

Hall, J. M., and Ryall, P. J. C., 1977. Paleomagnetism of basement rocks, Leg 37. *In* Aumento, F., Melson, W. G., et al., *Init. Repts. DSDP*, 37: Washington (U.S. Govt. Printing Office), 425-448.

Klitgord, K. D., Huestis, S. P., Mudie, J., D., and Parker, R. L., 1975. An analysis of near-bottom magnetic anomalies: Sea-floor spreading and the magnetized layer. *Geophys. J. R. Astron. Soc.*, 43:387-424.

Klitgord, K. D., and Mudie, J. D., 1974. The Galapagos spreading centre: A near-bottom geophysical survey. *Geophys. J. R. Astron. Soc.*, 38:563-586.

Levi, S., 1980. Paleomagnetism and some magnetic properties of basalts from the Bermuda Triangle. *In* Donnelly, T., Francheteau, J., Bryan, W., Robinson, P., Flower, M., Salisbury, M., et al., *Init. Repts. DSDP*, 51, 52, 53, Pt. 2: Washington (U.S. Govt. Printing Office), 1363-1378.

Levi, S., Bleil, U., Smith, B. M., and Rigotti, P. A., 1980. Compilation of paleomagnetic and rock magnetic results of basalt samples from Deep Sea Drilling Project Legs 51, 52, and 53. *In* Donnelly, T., Francheteau, J., Bryan, W., Robinson, P., Flower, M., Salisbury, M., et al., *Init Repts. DSDP*, 51, 52, 53, Pt. 2: Washington (U.S. Govt. Printing Office), 1337-1350.

Lowrie, W., 1977. Intensity and direction of magnetization in oceanic basalts. *J. Geol. Soc. London*, 133:61-82.

Marshall, M., 1978. The magnetic properties of some DSDP basalts from the North Pacific and inferences for Pacific plate tectonics. *J. Geophys. Res.*, 83:289-308.